

Shape Memory Alloy Bolted Joint for Medical Application by Finite Element Method

Yanping Wang

College of Medicine, Xi'an International University, Xi'an, People's Republic of China
375031254@qq.com

Abstract: Shape memory alloy (SMA) have shown excellent ability for medical application. In this research, a three-dimensional SMA constitutive model with superelastic character is proposed based on the framework of general inelasticity and implemented successfully into the finite element software (e.g. ANSYS). The effectiveness of such implementation is verified by the experimental results of superelastic NiTi alloy taken from the literature. Finally, the stress distribution of a bolted joint for osteopathic medicine is analyzed by this model.

Keywords: Shape Memory Alloys, Superelasticity, Bolted Joint

1. Introduction

SMA's are used in many domains including automotive, aerospace, robotic and biomedical and other medical device and equipment [1]. Some researchers had worked on the implementation of constitutive model of SMA into finite element codes [2-4]. A superelastic constitutive model proposed by Auricchio [2] had been implemented successfully into the finite element softwares, such as ANSYS and ABAQUS. In this paper, a three-dimensional phenomenological constitutive model with temperature dependent feature is developed under the framework of the generalized plasticity to describe the thermo-mechanical deformation of superelastic SMA. Finally, a numerical example is given to verify the effectiveness of the implementation, and applied to the analysis of the stress distribution of a bolted joint. The prediction capability of the proposed model is proved by the experiment results.

2. Constitutive Modeling

Generalized plasticity theory is firstly proposed by Saint-Sulpice [5] to depict the thermo-mechanical response of SMA's, which is based on the local internal variable theory considering the rate-independent inelastic behavior primarily based on the irreversibility under loading and unloading. Under the assumption of the infinitesimal strain, the total strain $\tilde{\boldsymbol{\epsilon}}$ is additively decomposed into the elastic and inelastic strain ($\tilde{\boldsymbol{\epsilon}}_e$ and $\tilde{\boldsymbol{\epsilon}}_{in}$) yields:

$$\tilde{\boldsymbol{\epsilon}} = \tilde{\boldsymbol{\epsilon}}_e + \tilde{\boldsymbol{\epsilon}}_{in} \quad (1)$$

Under the small deformation assumption, the total inelastic strain $\tilde{\boldsymbol{\epsilon}}_{in}$ just is the stress induced martensitic transformation $\tilde{\boldsymbol{\epsilon}}_t$ in this paper. Therefore, the total strain expression is:

$$\tilde{\boldsymbol{\epsilon}} = \tilde{\boldsymbol{\epsilon}}_e + \tilde{\boldsymbol{\epsilon}}_{in} = \tilde{\boldsymbol{\epsilon}}_e + \tilde{\boldsymbol{\epsilon}}_t \quad (2)$$

After discretizing the equation, the expressions can be written as follows:

$$\Delta \tilde{\boldsymbol{\epsilon}}_{in} = \Delta \tilde{\boldsymbol{\epsilon}}_t \quad (3)$$

$$\Delta \tilde{\boldsymbol{\varepsilon}}_e = \Delta \tilde{\boldsymbol{\varepsilon}} - \Delta \tilde{\boldsymbol{\varepsilon}}_t \quad (4)$$

The stress induced martensite and its reverse transformation can be defined as the martensitic volume fraction as the internal variable $\tilde{\xi}$. Hence the elastic stress-strain relationship can be written as:

$$\tilde{\boldsymbol{\sigma}} = \tilde{\boldsymbol{\sigma}}^* - \tilde{\mathbf{D}}^e(\tilde{\xi}) : \Delta \tilde{\boldsymbol{\varepsilon}}_{in} \quad (5)$$

in which, $\tilde{\mathbf{D}}^e(\tilde{\xi})$ is the equivalent elastic tensor [6,8], and $\tilde{\mathbf{D}}^e(\tilde{\xi}) = [(1-\tilde{\xi})\tilde{\mathbf{D}}_A^{-1} + \tilde{\xi}\tilde{\mathbf{D}}_M^{-1}]^{-1}$. $\tilde{\mathbf{D}}_M$ and $\tilde{\mathbf{D}}_A$ are the elastic tensor of martensite and austenite, respectively. By considering the deviatoric stress of the Equation (5), it can be derived as $\tilde{\mathbf{D}}^e : \Delta \tilde{\boldsymbol{\varepsilon}}_{in} = 2\tilde{G}\Delta \tilde{\boldsymbol{\varepsilon}}_{in}$, and:

$$\tilde{\boldsymbol{s}} = \tilde{\boldsymbol{s}}^* - 2\tilde{G}\Delta \tilde{\boldsymbol{\varepsilon}}_{in} \quad (6)$$

in which, \tilde{G} is the shear elastic tensor, and $\tilde{\boldsymbol{s}}^*$ is the deviatoric stress tensor of $\tilde{\boldsymbol{\sigma}}^*$.

Some phase transformations are stress-dependent, as described in the references [9, 11]. To consider this effect, the Von-Mises typed transformation surface is set as:

$$\tilde{F}(\tilde{\boldsymbol{\sigma}}, q) = \tilde{\boldsymbol{\sigma}}_{eq} - \tilde{\boldsymbol{\sigma}}_y(q) = 0 \quad (7)$$

where $\tilde{\boldsymbol{\sigma}}_{eq} = \left[\frac{3}{2} \tilde{\boldsymbol{s}} : \tilde{\boldsymbol{s}} \right]^{\frac{1}{2}}$ is the von-Mises equivalent stress. The forward transformation and its reverse transformation are described as follows:

$$\tilde{F}_{AM}(\tilde{\boldsymbol{\sigma}}, q) = \tilde{\boldsymbol{\sigma}}_{eq} - \sigma_{s,T}^{AM}(\tilde{\xi}) = 0, \text{ forward transformation} \quad (8a)$$

$$\tilde{F}_{MA}(\tilde{\boldsymbol{\sigma}}, q) = \tilde{\boldsymbol{\sigma}}_{eq} - \sigma_{s,T}^{MA}(\tilde{\xi}) = 0, \text{ reverse transformation} \quad (8b)$$

where, $\sigma_{s,T}^{AM}$ and $\sigma_{s,T}^{MA}$ are the forward and reverse transformation for the start stresses, respectively.

In this research, the transformation strain $\tilde{\boldsymbol{\varepsilon}}_t$ can be correlated to the martensite volume fraction $\tilde{\xi}$ by the following equation:

$$\tilde{\xi} = \tilde{\boldsymbol{\varepsilon}}_t / \varepsilon_L \quad (9)$$

in which, ε_L is the maximum uniaxial tension phase transformation strain. This parameter can be obtained by the experiments under loading-unloading. Similar to the classical plactical theory, the transformation strain rate complied with the normality rule in the stress space, i.e., it is normal to the transformation stress surface as

$$\Delta \tilde{\boldsymbol{\varepsilon}}_t^{AM} = \sqrt{\frac{3}{2}} \varepsilon_L \Delta \tilde{\xi} \mathbf{n}_{AM}, \Delta \tilde{\xi} > 0, \text{ forward phase transformation} \quad (10a)$$

$$\Delta \tilde{\boldsymbol{\varepsilon}}_t^{MA} = \sqrt{\frac{3}{2}} \varepsilon_L \Delta \tilde{\xi} \mathbf{n}_{MA}, \Delta \tilde{\xi} < 0, \text{ reverse phase transformation} \quad (10b)$$

with

$$\mathbf{n}_{AM} = \frac{\partial \tilde{F}_{AM}(\tilde{\boldsymbol{\sigma}}, \tilde{\xi})}{\partial \tilde{\boldsymbol{\sigma}}} = \sqrt{\frac{3}{2}} \frac{\tilde{\mathbf{s}}}{\tilde{\boldsymbol{\sigma}}_{eq}} \quad (11a)$$

$$\mathbf{n}_{MA} = \frac{\partial \tilde{F}_{MA}(\tilde{\boldsymbol{\sigma}}, \tilde{\xi})}{\partial \tilde{\boldsymbol{\sigma}}} = \sqrt{\frac{3}{2}} \frac{\tilde{\mathbf{s}}}{\tilde{\boldsymbol{\sigma}}_{eq}} \quad (11b)$$

In this research, the austenitic and martensitic phase transformation at different temperature is considered under the implicit stress integral solution.

Based on the implicit stress integration method, the isotropic elastic and plastic constitutive model is extended to that of the constitutive model of SMA. According to the above assumption, for the implicit stress integration of the phase change process, Equation (6) can be further written as follows:

$$\tilde{\mathbf{s}} = \tilde{\mathbf{s}}^* - 2\tilde{G}\Delta\tilde{\boldsymbol{\varepsilon}}_t \quad (12)$$

Equations (10a-b) can be rewritten as:

$$\Delta\tilde{\boldsymbol{\varepsilon}}_t^{AM} = \sqrt{\frac{3}{2}}\varepsilon_L\Delta\tilde{\xi}\tilde{\mathbf{n}}_{AM}, \Delta\tilde{\xi} > 0, \text{ forward phase transformation} \quad (13a)$$

$$\Delta\tilde{\boldsymbol{\varepsilon}}_t^{MA} = \sqrt{\frac{3}{2}}\varepsilon_L\Delta\tilde{\xi}\tilde{\mathbf{n}}_{MA}, \Delta\tilde{\xi} < 0, \text{ reverse phase transformation} \quad (13b)$$

3. Verification of Proposed Model

To prove the validity of the proposed model, the superelastic stress-strain curve at different temperature is simulated by using the parameters presented as follows:

$E_A^{T_0} = 41.0\text{GPa}$, $E_M^{T_0} = 37.0\text{GPa}$; $\nu_A = \nu_M = 0.33$; $C_{AM} = 8.0\text{MPa/K}$, $C_{MA} = 8.8\text{MPa/K}$; $k = 0.16$;
 $\sigma_{s,T_0}^{AM} = 353.0\text{MPa}$, $\sigma_{f,T_0}^{AM} = 381.0\text{MPa}$, $\sigma_{s,T_0}^{MA} = 141.0\text{MPa}$, $\sigma_{f,T_0}^{MA} = 122.0\text{MPa}$; $\varepsilon_L = 0.035$; $T_0 = 295\text{K}$;
 $h_M^p = 6.7\text{GPa}$.

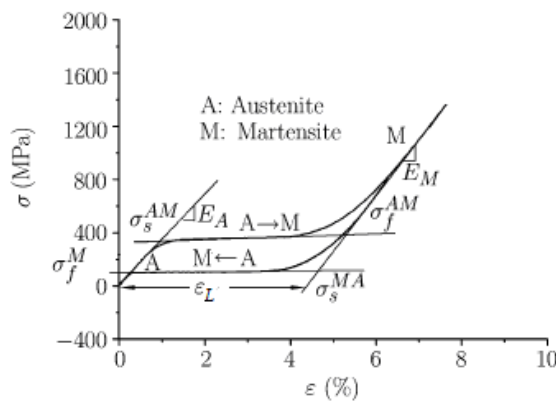


Fig.1. Phase change and plasticity behavior diagram of SMA

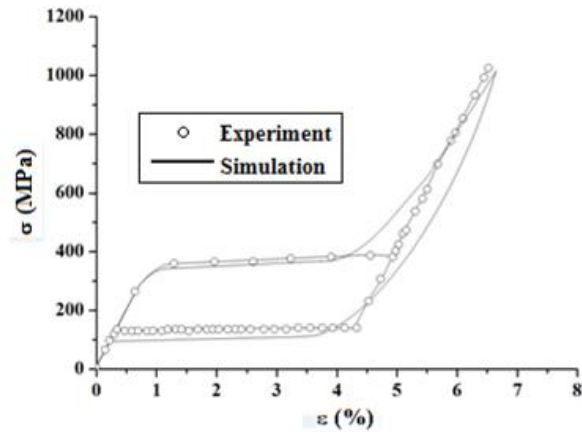


Fig.2. Uniaxial tension and unloading of NiTi shape memory alloy with phase transformation

The uniaxial loading-unloading of the SMA material is calculated with the proposed model. The result of the phase transformation simulation is compared with the experiment by Kang [12]. The simulational result is shown in Figure 2. It can be observed from Figure 2 the stress induced martensitic change. As the load is enough to reach the start stress $\sigma_{s,T}^{AM}$ of phase change, the martensite will take place. And then as the load is enough to unload the stress to reach the finish stress $\sigma_{f,T}^{MA}$ of phase change, the austenite will occur as following. The initial elastic loading curve is coincident with the elastic unloading one. It can be observed from Figure 2 that the response peak stress reach approximately 1800Mpa. The simulated results show good consistent with the experimental ones. The results show that the proposed model can effectively predict the superelastic phenomenon of the SMA. It can be concluded that the model can also offer a reasonable prediction under other working condition within the temperature range.

4. Finite Element Analyses for the SMA Bolted Joint

In this section, the proposed constitutive model is used to be carried out to analyze the stress distribution of a bolted joint. The mesh model is in Figure 3. Because the SMA bolted joint structure is a spatial axisymmetric structure, only the section map is selected to establish the finite element model in this research to simulate the stress distribution of the bolted joint under the axial bolted preload. The type of element is set four-noded plane element 182 with the isotropic character. The Young's modulus of members is set as 209GPa, and the Poisson's ratio is 0.3. The contact surface element CONTA172 and the target surface element TARGE169 are used to generate contact pairs of the finite element model. The bolt pretightening element Prets179 is used to produce the preloading force of the bolt.

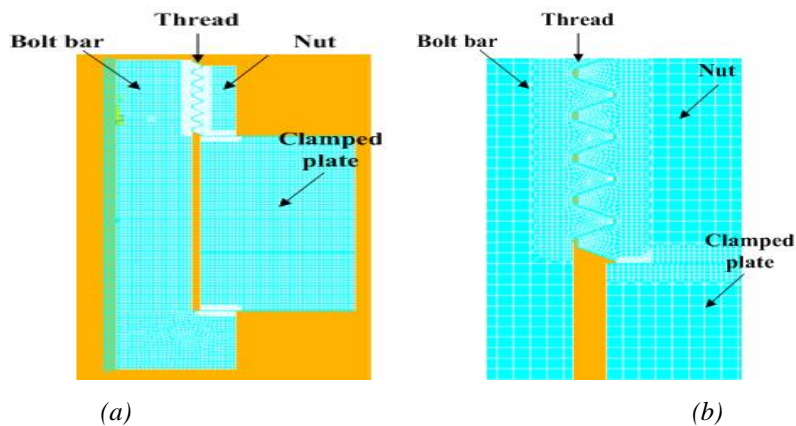


Fig.3. Two-dimensional mesh model of bolted joint: (a) Overall model, (b) Local refined model

In this study, the finite element model of bolt is in first preloaded and unloaded. The equivalent stress cloud chart of the finite element model after calculation is observed, as shown in Figures 4 (a)

and (b). The two stress cloud maps correspond to the A and B points of the stress-strain curve of the node 1, as shown in Figure 5 (a). The A point indicates the end time of martensitic transformation, but no plastic deformation occurs. When the load continues to reach the B point, it indicates that the plastic deformation has occurred and the peak stress is 1746MPa. Because the peak stress is higher than the plastic yield stress of martensite, the plastic deformation of superelastic NiTi alloy continues to occur after the martensite elastic deformation, and the deformation goes through three stages. Due to the plastic deformation of martensite, some residual deformation will be produced after unloading. This part of the deformation can not be recovered after unloading, which leads to the lose of the superelastic part of the NiTi alloy. The stress strain curve of node 2 shown in Figure 5 (b) shows that the stress concentration of bolt screw thread is more relieved than the stress concentration in the load part of the nut, which is far from the martensitic plastic yield point. However, it can be found an obvious superelasticity. When the bolt preload is unloaded, the stress returns to the initial zero point. From the above discussions, the results of the ANSYS simulation based on the proposed model are in good agreement with the the uniaxial tensile test results of SMA, which also shows that the finite element implementation of the constitutive model is valid.

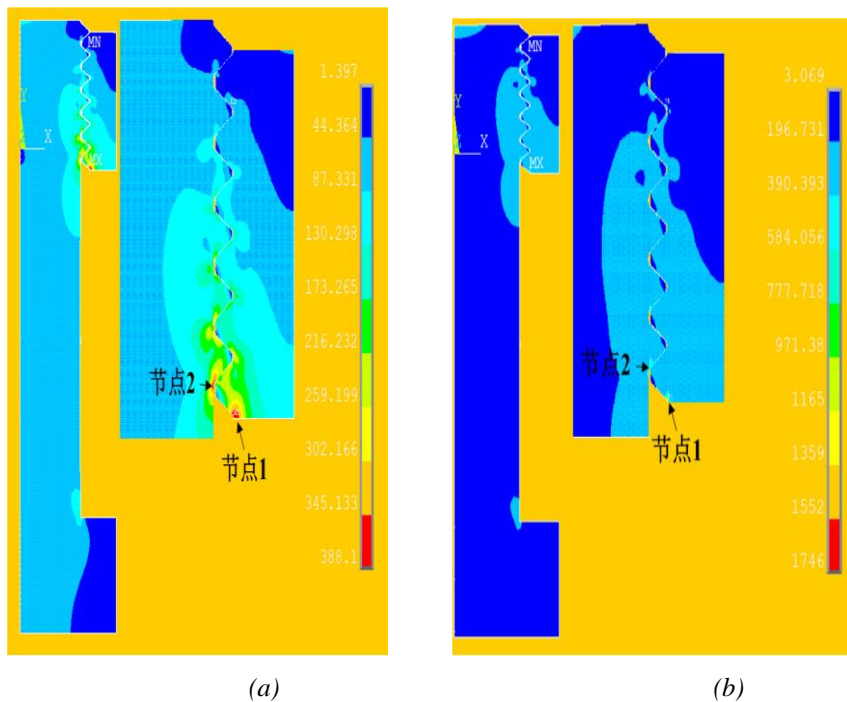


Fig.4. (a) Equivalent stress cloud map at the end of martensitic phase transition, (b) Equivalent stress cloud map at martensitic plastic yield moment

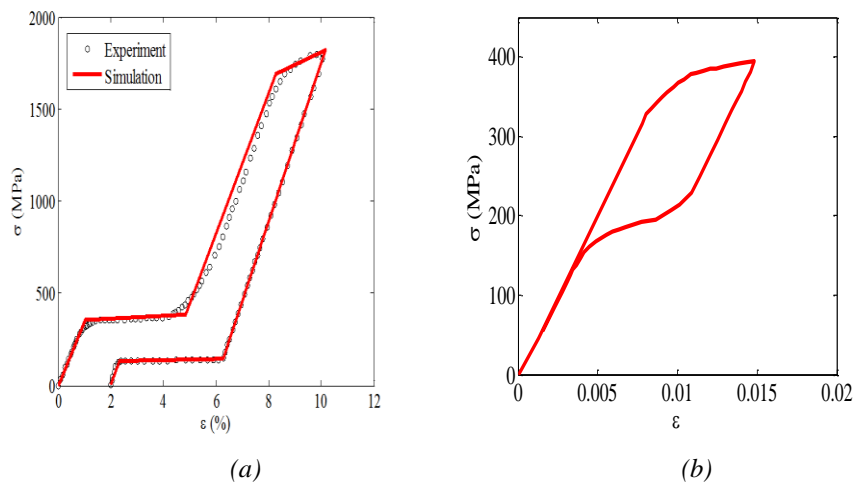


Fig.5. (a) Stress-strain curve of node 1 at different times, (b) Stress-strain curve of node 2 at different times

5. Conclusions

In this paper, it is proposed a SMA constitutive model in the general inelastic framework considering the implementation into the finite element software ANSYS. The numerical result shows the good simulation result under comparing with the experimental one. Finally, the numerical analysis for the SMA bolted joint presents the reasonable stress distribution and stress-strain curve of different node at different times.

Acknowledgments

This research was funded by National Natural Science Foundation of China grant number [51775406]; Special scientific research plan of Shaanxi Provincial Department of education in 2019 grant number [19JK0725]; and Fundamental Research Funds for the Central Universities grant number [JB180412].

References

- [1] J.M. Jani, M. Leary, A. Subic, "A review of shape memory alloy research, applications and opportunities", *Mater. Design.*, vol. 56, pp.1078–1113, 2014.
- [2] F. Auricchio, R.L. Taylor, "Shape-memory alloy modeling and numerical simulations of the finite-strain superelastic behavior," *Comput. Method Appl. Mech. Eng.*, vol.143, pp.175-194, 1997.
- [3] F. Auricchio, "A robust integration algorithm for a finite strain shape memory alloy superelastic model," *Int. J. Plasticity*, vol. 17, pp. 971-990, 2001.
- [4] N. Rebelo, M. Hsu, H. Foadian, "Simulation of superelastic alloys behavior with abaqus," *Proc. Int. Conf. on Shape memory and Superelastic Technologies. SMST, Pacific Grove (USA, 2001)*, pp. 457-469, 2000.
- [5] L. Saint-Sulpice, S.A. Chirani, S. Calloch, "A 3D superelastic model for shape memory alloys taking into account progressive strain under cyclic loadings," *Mech. Mater.*, vol. 41, pp.12-26, 2009.
- [6] Y. Ivshin, T. Pence, "A thermomechanical model for a one variant shape memory material," *J. Intel Mat. Syst Str.*, vol. 5, pp.455-473, 1994.
- [7] F. Auricchio, S. Marfia, E. Sacco, "Modelling of SMA materials: Training and two way memory effects," *Comp. Struct.*, vol. 81, pp.2301-2317, 2003.
- [8] W. Zaki, Z. Moumni, "A 3-D model of the cyclic thermomechanical behavior of shape memory alloys," *J Mech. Phys. Solids.*, vol. 55, pp.2427-2454, 2007.
- [9] C. Liang, C. Rogers, "One-dimensional thermomechanical constitutive relations for shape memory materials," *J. Intel Mat. Syst Str.*, vol. 1, pp.207-234, 1990.
- [10] F. Auricchio, E. Sacco, "A one-dimensional model for superelastic shape memory alloys with different elastic properties between austenite and martensite," *Int. J Nonlin. Mech.*, vol. 32, pp.1101-1114, 1997.
- [11] X.J. Jiang, B.T. Li, "Finite element analysis of a superelastic shape memory alloy considering the effect of plasticity," *J. Theor. App. Mech.*, vol. 55(4), pp.1355-1368, 2017.
- [12] G.Z. Kang, Q.H. Kan, L.M. Qian, "Ratchetting deformation of superelastic and shape-memory NiTi alloys," *Mech. Mater.*, vol. 41, pp.139-153, 2009.